Tuijin Jishu/Journal of Propulsion Technology
ISSN: 1001-4055
Vol. 44 No. 4 (2023)

Analysis Of Two-Layered Model Of Blood Flow Through Stenosed Tube With Permeable Walls In The Presence Of Magnetic Field Considering Blood As Couple Stress Fluid With Variable Viscosity And Slip Velocity

[1]Neha Phogat, [2]Sumeet Gill, [3]Rajbala Rathee, [4]Jyoti

[1][4] Research Scholar, Deptt. of Mathematics, M.D. University, Rohtak-124001, Haryana, India
[2]Professor, Deptt. of Mathematics, M. D. University, Rohtak-124001, Haryana, India
[3] Assistant Professor, A.I.J.H. Memorial College, Rohtak-124001, Haryana, India

Abstract: The paper investigates the "two-layered model of blood flow" as steady incompressible couple stress fluid through one-dimensional channel in multi-stenosed blood vessel. Within the core region, the blood flow is conceptualized as a dynamic entity exhibiting the attributes of a couple stress fluid, distinguished by variable viscosity orchestrated in accordance with the precepts delineated by the Einstein relation and the peripheral region of the tube comprises of plasma which is considered as "Newtonian fluid with constant viscosity". The governing equations of the blood flow are solved using the Frobenius technique using the slip boundary condition and the expressions are derived for peripheral and central velocities along with shear stress and pressure gradient. The effects of various parameters on the flow variables have been emphasised. MATLAB programming software is used to visualize the results regarding shear stress and pressure gradient. The study further interrogates the effect of change in thickness of peripheral layer on pressure gradient under the influence of magnetic field and slip velocity.

Keywords: Einstein relation, slip velocity, magnetic field, shear stress, frobenius technique, pressure gradient.

1. Introduction

The complex dynamics of blood flow within the circulatory system have long been a subject of intense research due to their paramount importance in understanding cardiovascular diseases and optimizing medical interventions. Hemodynamics, the study of blood flow in the circulatory system, plays a crucial role in elucidating the intricate phenomena associated with blood transport through vessels of varying geometries and properties. The flow of blood within stenosed tubes, which are constrictions or narrowings in blood vessels, is of particular interest due to its clinical relevance in conditions such as atherosclerosis, thrombosis, and other vascular diseases. Misra et al. [1] introduced a "non-newtonian" model of blood flow through confined arteries. A couple stress fluid model is characterized by its ability to account for the rotational deformations that occur within blood at the microscale. Blood is not a homogeneous, continuous fluid but rather comprises discrete components, including red and white blood cells, platelets, and plasma. These components interact and deform in response to fluid shear, exhibiting complex behavior. Modeling blood as a couple stress fluid allows us to capture these intricate microstructural effects [10].

Magnetic fields have emerged as a non-invasive tool with the potential to manipulate blood flow within the circulatory system. This area of research holds promise for novel diagnostic and therapeutic approaches. Magnetic fields can be applied externally, offering a means to exert control over the movement of blood without the need for invasive procedures. One significant application of magnetic fields in hemodynamics is the control of drug delivery. Magnetic nanoparticles, when introduced into the bloodstream, can be directed to specific target sites using external magnetic fields [2]. This technique has opened up possibilities for precisely delivering therapeutic agents to diseased tissues, reducing side effects, and enhancing treatment efficacy. Additionally, magnetic fields have been explored for their potential to enhance targeted drug delivery within the circulatory system [3]. The ability to guide therapeutic agents to specific regions of the vascular network offers considerable potential for improving the treatment of vascular diseases and cancers. Further, the impact of slip velocity against

the wall in a blood flow was investigated by Roy and Sinha [4]. Kumari et al. [5] diagnosed the peristaltic flow properties of blood through stenotic artery in the presence of magnetic field and slip velocity. The model for peculiar arterial expansion because of "intravascular plaques" is characterized in figure 1.

The present study takes into account the presence of magnetic fields, and models blood as a couple stress fluid with variable viscosity and slip velocity. These complex factors interplay in a way that significantly influences the flow patterns and transport properties of blood within the circulatory system. Understanding these dynamics not only provides insight into the fundamentals of blood flow but also has important implications for clinical diagnostics and treatment strategies.

2. Formulation of the Problem:

We examine a scenario involving a continuous, incompressible, and extensively matured blood flow with a viscosity that changes as it courses through the central stratum within a dual-layer framework representing the dynamics of blood circulation in a constricted artery. The geometry of this complex, narrowed arterial passage is

$$R_1(z) = \begin{cases} \alpha R_0 - \frac{2\delta_1}{L_0}(z-d), & d \le z \le d + \frac{L_0}{2} \\ \alpha R_0 - \frac{\delta_1}{L_0}\left\{1 + cos\frac{2\pi}{L_0}\left(z - d - \frac{L_0}{2}\right)\right\}, & d + \frac{L_0}{2} \le z \le d + L_0 \\ \alpha R_0, & otherwise \end{cases} \quad (1)$$

$$R(z) = \begin{cases} R_0 - \frac{2\delta_s}{L_0}(z-d), & d \le z \le d + \frac{L_0}{2} \\ R_0 - \frac{\delta_s}{L_0}\left\{1 + cos\frac{2\pi}{L_0}\left(z - d - \frac{L_0}{2}\right)\right\}, & d + \frac{L_0}{2} \le z \le d + L_0 \\ R_0, & \end{cases} \quad (2)$$

where $R_1(z)$ and $R(z)$ are respectively the "radii of central layer and stenotic tube with peripheral layer", and R_0 is the "radius of unobstructed blood vessel". L_0 is the length of the tube, d is the position of stenosis, δ_s is the height of stenosis, δ_1 is the maximum bulging of the interface at $z = d + \frac{L_0}{2}$, α is the ratio of radius to central layer and radius of unobstructed artery.

The viscosity of the blood within the central layer is permitted to fluctuate in accordance with the principles outlined by the Einstein relation

$$\mu_c = \mu_p[1 + \beta h(r)] \quad (3)$$

where μ_c is "viscosity of central layer", μ_p is "viscosity of plasma", $h(r)$ is "hematocrit" and β is constant.

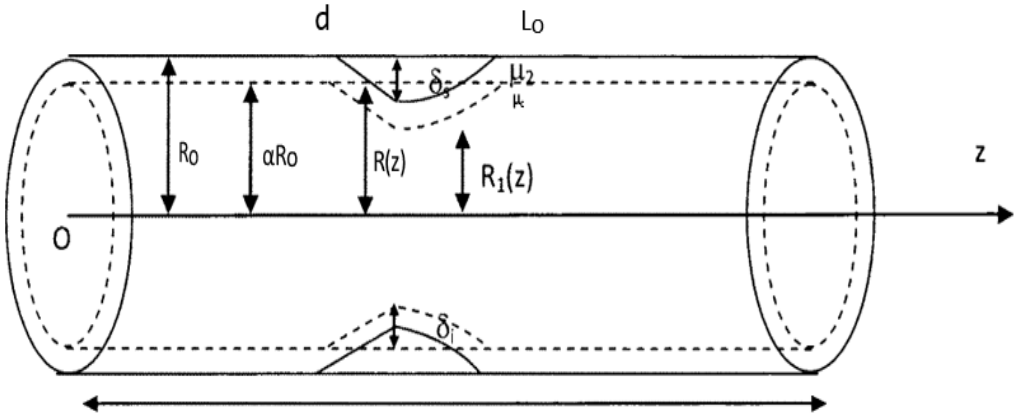

Figure 1

Hematocrit is described as by the relation

$$h(r) = h_m\left[1 - \left(\frac{r}{R_0}\right)^3\right] \tag{4}$$

where h_m is "maximum hematocrit of blood" and R_0 is "radius of unstenosed artery".

Substituting the value of $h(r)$ from equation (4) in equation (3), we get

$$\mu_c = \mu_p\left[a - k\left(\frac{r}{R_0}\right)^3\right] \tag{5}$$

where $a = 1 + k$ and $k = \beta h_m$.

In this particular problem, we investigate the behaviour of blood flow that adheres to a non-Newtonian pattern within the innermost stratum of a two-layer construct that simulates blood circulation. The fluid occupying the core region of the conduit is characterized as a couple stress fluid, while the outermost layer of the blood vessel contains plasma, conforming to the characteristics of a constant viscosity Newtonian fluid. The governing equations dictating the flow dynamics within both the central and peripheral layers in this present scenario are articulated as follows

$$\mu_c\nabla^2\mu_c - \eta\nabla^4\mu_c + \left(\frac{\partial\mu_c}{\partial r}\right)\left(\frac{\partial u_c}{\partial r}\right) - \beta_0^2\sigma_e^c u_c - \frac{\partial p}{\partial z} = 0 \tag{6}$$

$$\mu_p\nabla^2\mu_p - \beta_0^2\sigma_e^p u_p - \frac{\mu_p}{K}u_p - \frac{\partial p}{\partial z} = 0 \tag{7}$$

where $\frac{\partial p}{\partial z}$ is the pressure gradient, K is the "permeability constant", η is the "couple stress constant", u_c and u_p are the fluid velocities, σ_e^c and σ_e^p are "electrical conductivities for central and peripheral layers", accordingly.

The boundary conditions are described as

$\frac{\partial u}{\partial r} = -hu$ (Slip condition)

or

$u' + hu = 0$ when $r = R$ (8)

where $h = -\frac{\eta_1}{R_o\sqrt{K}}$; η_1 is constant which depends on the properties of "porous medium" and on its structure.

$\frac{\partial^2\mu_c}{\partial r^2} - \frac{\eta}{r}\frac{\partial\mu_c}{\partial r} = 0$ at $r = R_1(z)$ (9)

$\frac{\partial u_c}{\partial r} = 0$ at $r = 0$ (10)

$u_c = u_p$ at $r = R_1(z)$ (11)

$\tau_c = \tau_p$ at $r = R_1(z)$ (12)

Considering the transformation,

$x = \frac{r}{R_0}$

to make the variable r dimensionless.

So, the governing equations (6) and (7) becomes,

$$(a - kx^3)\left[x^3\frac{\partial^2 u_c}{\partial x^2} + x^2\frac{\partial u_c}{\partial x}\right] - 3kx^5\frac{\partial u_c}{\partial x} - \frac{1}{\alpha_1^2}\left[x^3\frac{\partial^4 u_c}{\partial x^4} + 2x^2\frac{\partial^3 u_c}{\partial x^3} - x\frac{\partial^2 u_c}{\partial x^2} + \frac{\partial u_c}{\partial x}\right]$$

$$-M_1^2x^3u_c = x^3\frac{R_0^2}{\mu_p}\frac{dp}{dz} \tag{13}$$

where α_1 is couple stress parameter, $\alpha_1^2 = \frac{\mu_p}{\eta}R_0^2$ and $M_1^2 = \frac{\beta_0^2R_0^2\sigma_e^c}{\mu_o}$ is the Hartmann number for central layer.

$$x\frac{\partial^2 u_p}{\partial x^2} + \frac{\partial u_p}{\partial x} - M_2^2 x u_p - \frac{R_0^2}{K}xu_p = x\frac{R_0^2}{\mu_p}\frac{dp}{dz} \tag{14}$$

where $M_2^2 = \frac{\beta_0^2R_0^2\sigma_e^p}{\mu_0}$ is the Hartmann number for peripheral layer.

Now, boundary condition becomes

$\frac{\partial^2\mu_c}{\partial x^2} - \frac{\eta}{x}\frac{\partial\mu_c}{\partial x} = 0$ at $x = \frac{R_1(z)}{R_0}$ (15)

$$\frac{\partial u_c}{\partial x} = 0 \qquad \text{at} \qquad x = 0 \tag{16}$$

$$u_p = -h\frac{\partial u_p}{\partial x} \qquad \text{at} \qquad x = \frac{R(z)}{R_0} \tag{17}$$

$$u_c = u_p \qquad \text{at} \qquad x = \frac{R_1(z)}{R_0} \tag{18}$$

$$\tau_c = \tau_p \qquad \text{at} \qquad x = \frac{R_1(z)}{R_0} \tag{19}$$

We will solve the equation (13) and (14) by using Frobenius Method and by applying boundary conditions, the expressions for velocities u_c and u_p can be obtained as

$$\begin{aligned}
u_c = \frac{\alpha_1^2 R_0^2}{64\mu_o[a-k(R_1/R_o)^3]}\frac{dp}{dz}\Bigg[&\sum_{m=0}^{\infty}(m+4)(m+3-\eta_1)B_m\left(\frac{R_1}{R_o}\right)^{m+3}\sum_{m=0}^{\infty}m(m-1\\
&-\eta_1)A_m\left(\frac{R_1}{R_o}\right)^{m-1}\sum_{m=0}^{\infty}F_m\left(\frac{R_1}{R_o}\right)^{m}\\
&\times\left\{\sum_{m=0}^{\infty}mA_m\left(\frac{R_1}{R_o}\right)^{m-1}\sum_{m=0}^{\infty}\overline{A_m}x^{m+2}-\sum_{m=0}^{\infty}(m+2)\overline{A_m}\left(\frac{R_1}{R_o}\right)^{m+1}\sum_{m=0}^{\infty}A_m x^m\right\}\\
&+\sum_{m=0}^{\infty}(m)(m-1-\eta_1)A_m\left(\frac{R_1}{R_o}\right)^{m-1}\left\{\sum_{m=0}^{\infty}(m+4)B_m\left(\frac{R_1}{R_o}\right)^{m+3}\sum_{m=0}^{\infty}F_m\left(\frac{R_1}{R_o}\right)^{m}\right.\\
&\left.+\frac{16}{\alpha_1^2}\left(\sum_{m=0}^{\infty}(m+2)\overline{F_m}\left(\frac{R_1}{R_o}\right)^{m+1}\sum_{m=0}^{\infty}F_m\left(\frac{R_1}{R_o}\right)^{m}-\sum_{m=0}^{\infty}mF_m\left(\frac{R_1}{R_o}\right)^{m-1}\sum_{m=0}^{\infty}\overline{F_m}\left(\frac{R_1}{R_o}\right)^{m+2}\right)\right\}\\
&\times\left\{\sum_{m=0}^{\infty}(m+2)(m+1-\eta_1)\overline{A_m}\left(\frac{R_1}{R_o}\right)^{m+1}\sum_{m=0}^{\infty}A_m x^m\right.\\
&\left.-\sum_{m=0}^{\infty}(m)(m-1-\eta_1)A_m\left(\frac{R_1}{R_o}\right)^{m-1}\sum_{m=0}^{\infty}\overline{A_m}x^{m+2}\right\}-\sum_{m=0}^{\infty}F_m\left(\frac{R_1}{R_o}\right)^{m}\sum_{m=0}^{\infty}m(m-1\\
&-\eta_1)A_m\left(\frac{R_1}{R_o}\right)^{m-1}\\
&\times\left\{\sum_{m=0}^{\infty}(m+2)(m+1-\eta_1)\overline{A_m}\left(\frac{R_1}{R_o}\right)^{m+1}\sum_{m=0}^{\infty}mA_m\left(\frac{R_1}{R_o}\right)^{m-1}\right.\\
&\left.-\sum_{m=0}^{\infty}m(m-1-\eta_1)A_m\left(\frac{R_1}{R_o}\right)^{m-1}\times\sum_{m=0}^{\infty}(m+2)\overline{A_m}\left(\frac{R_1}{R_o}\right)^{m+1}\right\}\sum_{m=0}^{\infty}B_m x^{m+4}\Bigg]\\
/\Bigg[&\sum_{m=0}^{\infty}(m)(m-1-\eta_1)A_m\left(\frac{R_1}{R_o}\right)^{m-1}F_m\left(\frac{R_1}{R_o}\right)^{m}\\
&\times\left\{\sum_{m=0}^{\infty}(m+2)(m+1-\eta_1)\overline{A_m}\left(\frac{R_1}{R_o}\right)^{m+1}\sum_{m=0}^{\infty}mA_m\left(\frac{R_1}{R_o}\right)^{m+1}-\sum_{m=0}^{\infty}(m)(m-1\right.\\
&\left.-\eta_1)A_m\left(\frac{R_1}{R_o}\right)^{m-1}\sum_{m=0}^{\infty}(m+2)\overline{A_m}\left(\frac{R_1}{R_o}\right)^{m+1}\right\}\Bigg]
\end{aligned} \tag{20}$$

$$u_p = \frac{R_o^2}{4\mu_0}\frac{dp}{dz}\frac{1}{\sum_{m=0}^{\infty} F_m \left(\frac{R}{R_o}\right)^m + h\sum_{m=0}^{\infty} mF_m \left(\frac{R}{R_o}\right)^{m-1}}\left[\sum_{m=0}^{\infty}\overline{F_m}\, x^{m+2}\sum_{m=0}^{\infty} F_m(\frac{R}{R_o})^m - \sum_{m=0}^{\infty} F_m\, x^m \sum_{m=0}^{\infty}\overline{F_m}(\frac{R}{R_o})^{m+2} + h\sum_{m=0}^{\infty}\overline{F_m}\, x^{m+2}\sum_{m=0}^{\infty} mF_m(\frac{R}{R_o})^{m-1} - h\sum_{m=0}^{\infty} F_m\, x^m \sum_{m=0}^{\infty}(m+2)\,\overline{F_m}(\frac{R}{R_o})^{m+1}\right] \quad (21)$$

3. Graphical Discussion

Using the MATLAB software, mathematical form of pressure gradient, and sheer stress at the walls of an artery are plotted for different values of slip parameter *h*, Hartman number M_1, M_2, permeability parameter K, couple stress fluid constant η and α_1 against stenosis size. Variation in pressure gradient due to increasing values of η, K, magnetic field and slip parameter are shown in the figure 2, 3, 4, 5 and 6. In Figure 2, as the stenosis size increases, the pressure gradient rises when α_1 is small, but it remains relatively stable as the stenosis size grows larger. When the stenosis size is held constant, the pressure gradient decreases significantly for α_1 values of 2 and 4, but it begins to increase again for α_1 values of 6, 8, and 10.. From figure 3 to 6, pressure gradient increases with increasing stenosis size. In the figure 3 and 4, pressure gradient increases due to increasing value of η and K. Several psychological and haemodynamic changes occur in the body when pressure gradient rises. In the figure 5, pressure gradient falls with increasing magnetic field and pressure gradient almost tends to 0 for high intensity magnetic field. In the figure 6, pressure gradient decreases gradually with increasing value of sleep parameter. Also, introducing slip parameter potentially reduces sheer stress exerted on the endothelial lining of the arteries as shown in figure 11. Decrease in shear stress have implications for vascular health and endothelial integrity.

Elevated pressure gradient can contribute to cardiovascular issues over time. The augmentation of the pressure gradient can be managed by employing an appropriate magnitude of magnetic field intensity and adjusting the slip parameters at the arterial walls.

Figure 7 to figure 11 shows variation in shear stress for different values of η, α_1, M_1, M_2, Kand slip parameter. In figure 7, shear stress firstly decreases when α_1=2, 4, but its start increasing for α_1=6, 8, 10 and it is almost 0 for α_1=10. In the figure 8, shear stress increases gradually due to increase in the value of η, but more hike is there for η=2. Increasing shear stress is crucial for maintaining endothelial health. In the figure 9, shear stress increases due to increase in the value of "permeability parameter". Rise in shear stress for large values of permeability parameter is not so much rapid as shear stress rises for small values of permeability parameter. In the figure 10, shear stress decreases due to increase in the magnetic field. Increase in the shear stress can be controlled by introducing slip parameter and magnetic field. Hence, it is demonstrated that the magnetic field enhances blood circulation to a certain degree. This assertion is corroborated by the findings of Haldar and Ghosh [6].

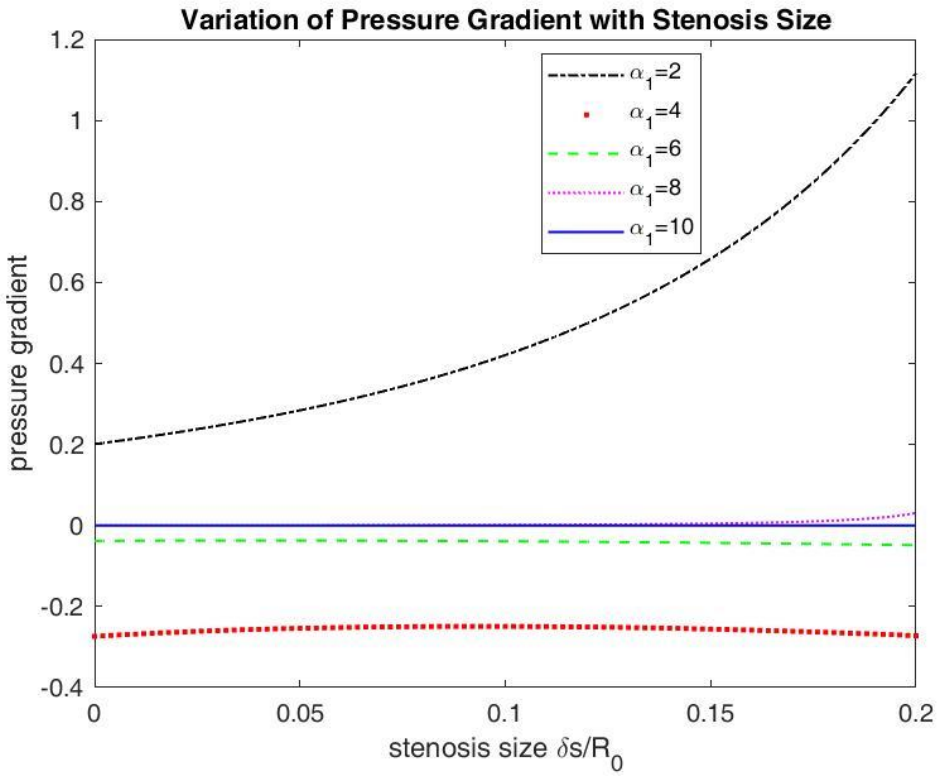

Figure 2

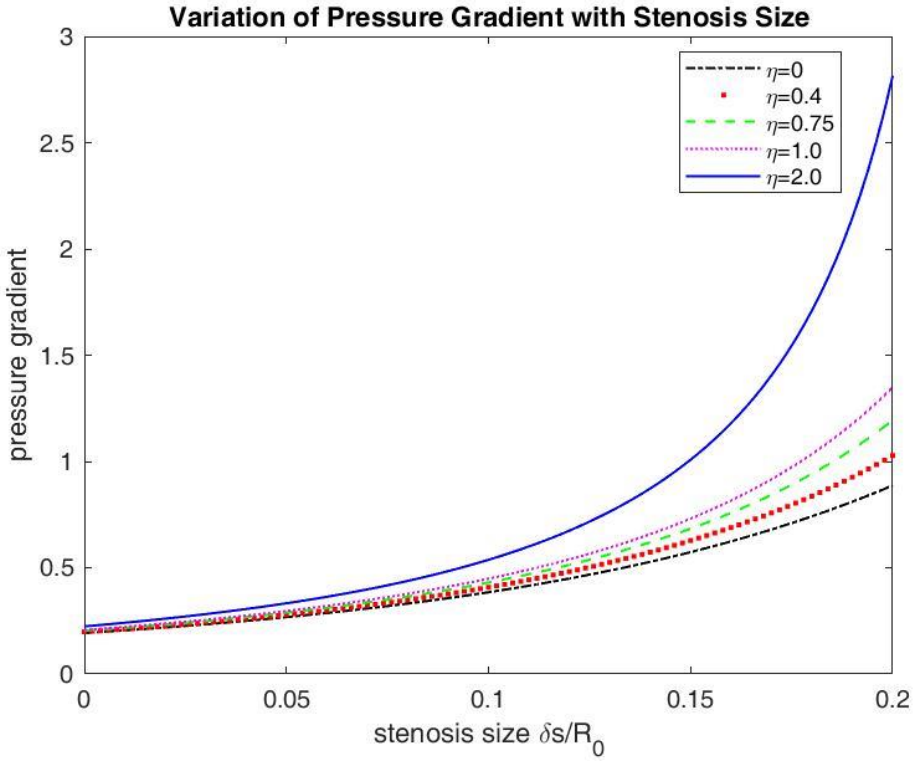

Figure 3

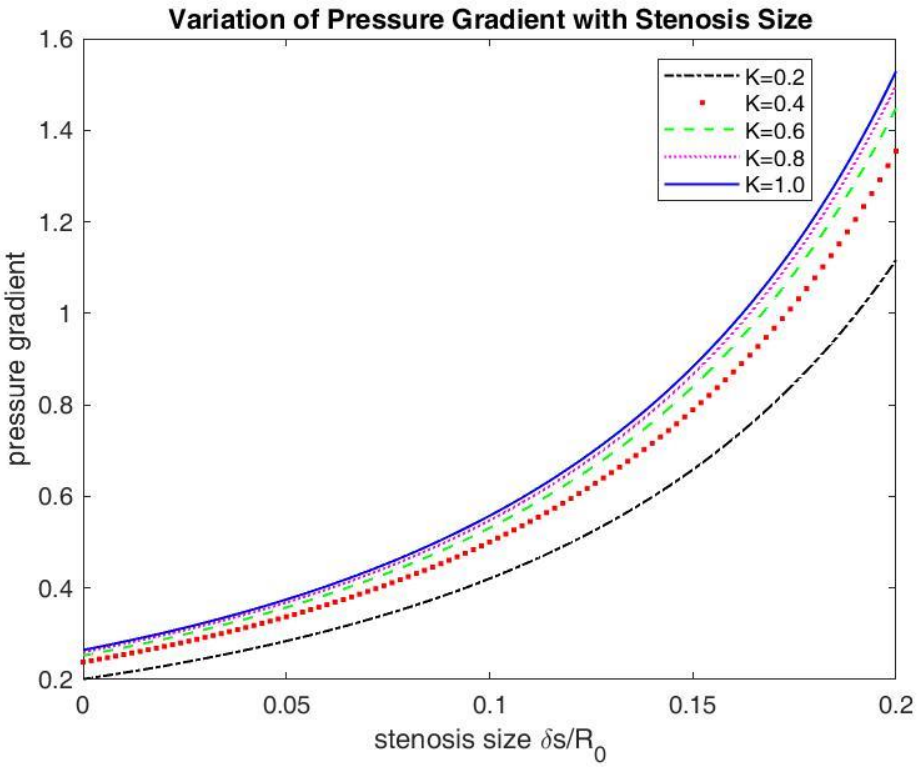

Figure 4

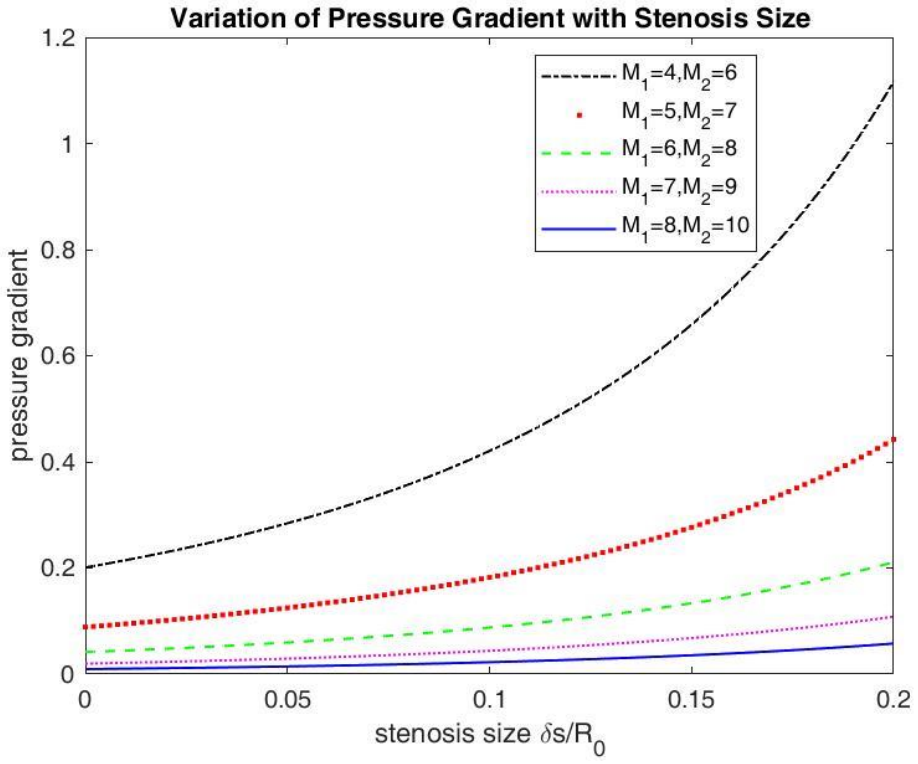

Figure 5

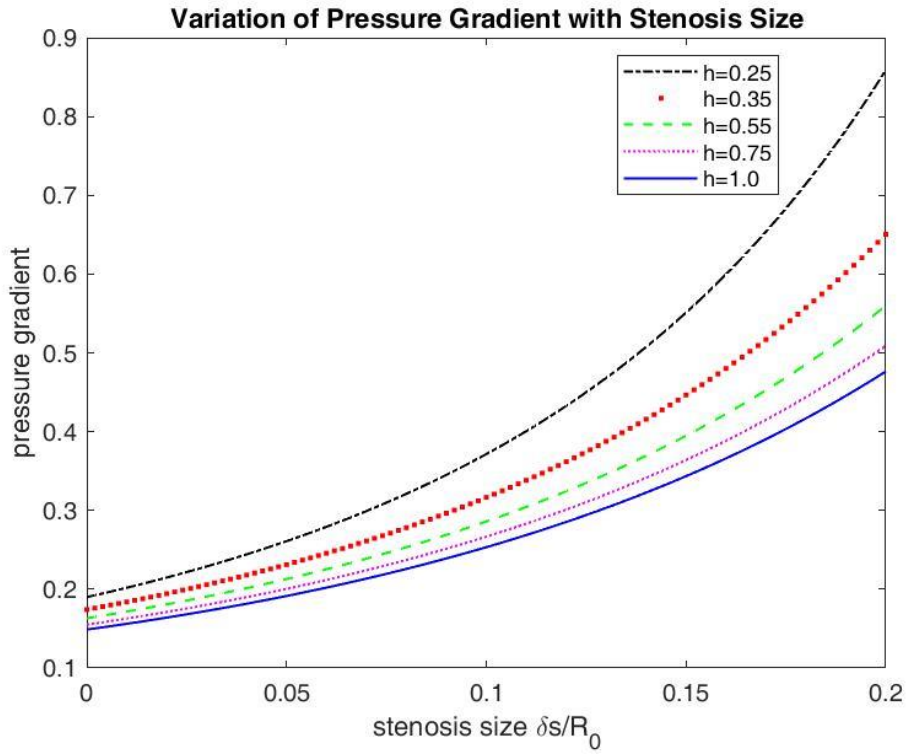

Figure 6

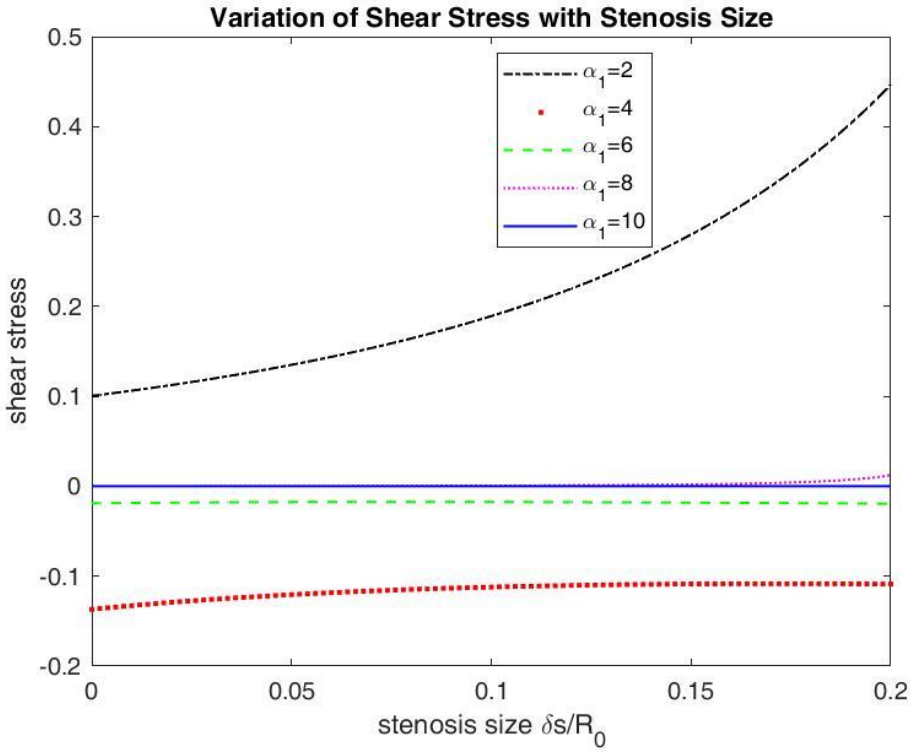

Figure 7

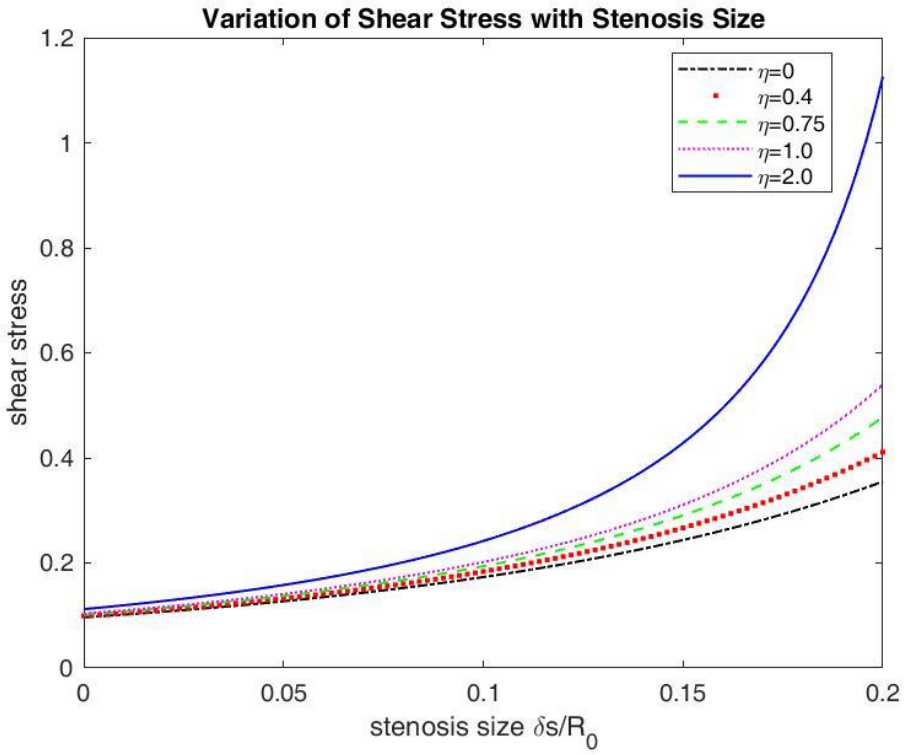

Figure 8

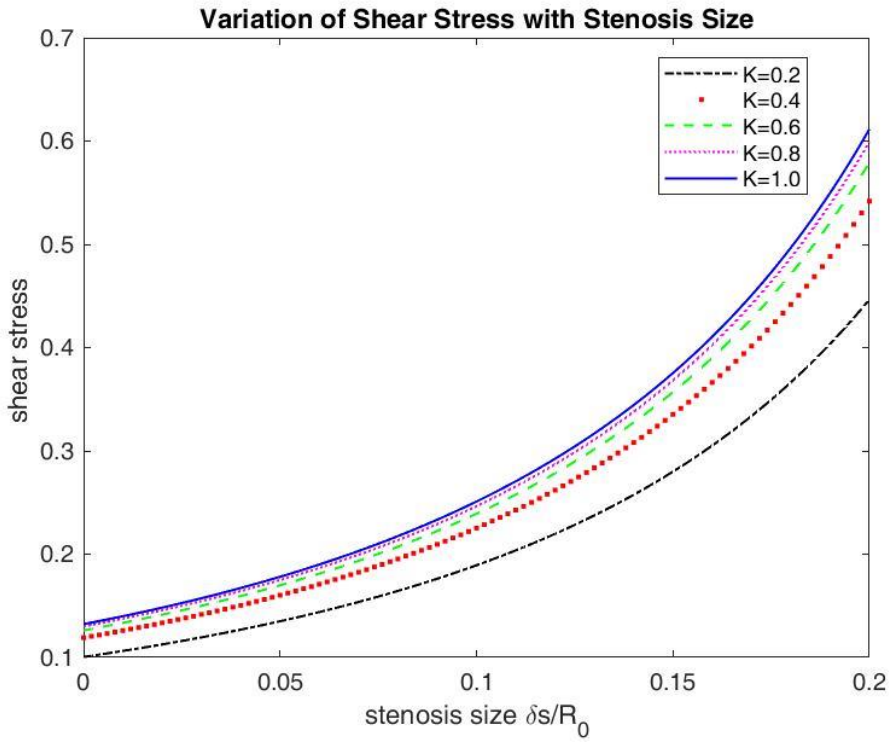

Figure 9

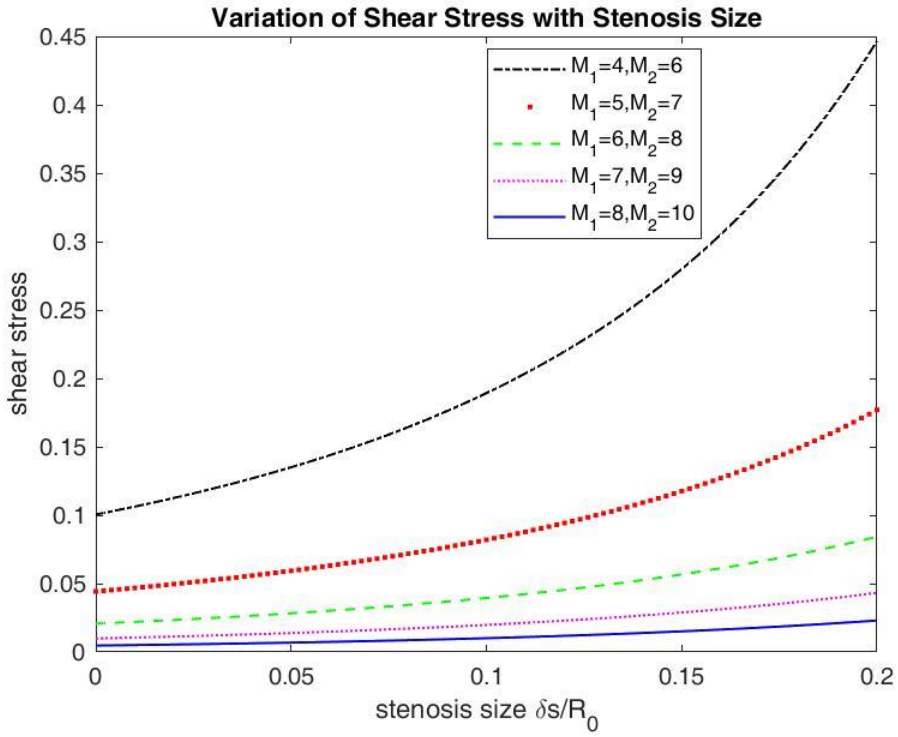

Figure 10

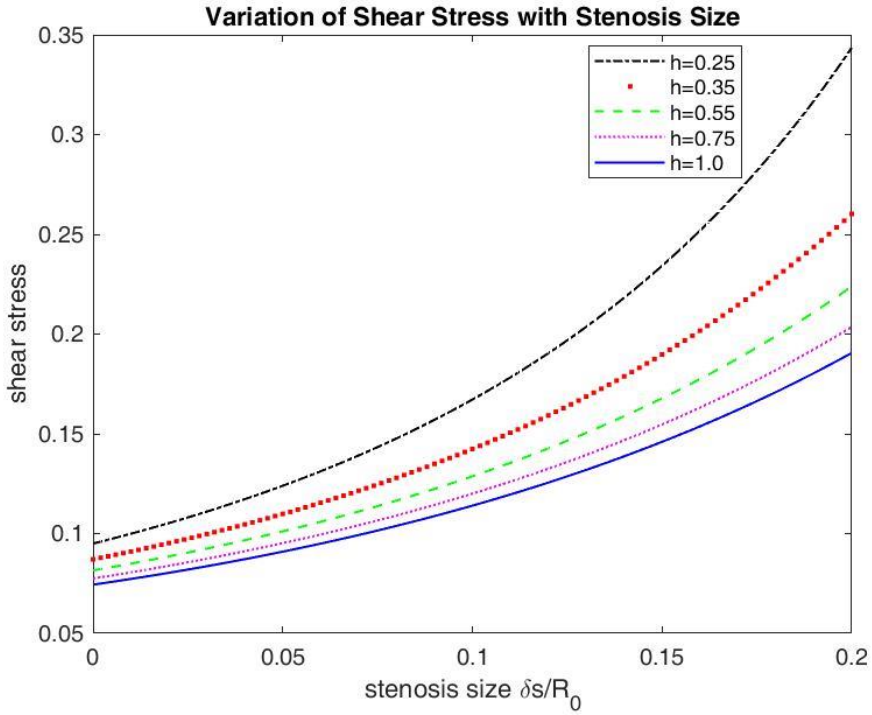

Figure 11

4. Conclusion

Blood flow through stenosed tubes is a multifaceted phenomenon with significant clinical relevance. The integration of magnetic fields, permeable walls, the characterization of blood as a couple stress fluid, and the consideration of variable viscosity and slip velocity adds layers of complexity to our understanding of this intricate flow behavior. The following are the significant findings of the study:

- When the pressure gradient decreases, flood of blow through blood vessels, slows down. This reduced blood flow can impact the delivery of oxygen and nutrients to the tissues and organs.
- When pressure gradient falls, heart may have to work harder to maintain adequate blood flow to the body that leads to complications. Changes in the blood flow pattern could impact the development and progression of stenosis or other vascular diseases.
- Changes in the shear stress can impact platelet behaviour and coagulation.
- Altered sheer stress might increase the risk of thrombus formation and clotting.

References

[1] Misra, J. C., Patra, M. K., & Misra, S. C. (1993). A non-Newtonian fluid model for blood flow through arteries under stenotic conditions. Journal of biomechanics, 26(9), 1129-1141.
[2] Pankhurst, Q. A., Connolly, J., Jones, S. K., & Dobson, J. (2003). Applications of magnetic nanoparticles in biomedicine. Journal of physics D: Applied physics, 36(13), R167.
[3] Liu, D., Poon, C., Lu, K., He, C., & Lin, W. (2014). Self-assembled nanoscale coordination polymers with trigger release properties for effective anticancer therapy. Nature communications, 5(1), 4182.
[4] Shit, G. C., Roy, M., & Sinha, A. (2014). Mathematical modelling of blood flow through a tapered overlapping stenosed artery with variable viscosity. Applied Bionics and Biomechanics, 11(4), 185-195.
[5] Kumari, S., Rathee, R., & Nandal, J. Peristaltic Flow Characteristics of Blood through Stenotic Artery under the influence of Magnetic Field and Slip Velocity.
[6] Haldar K. and Ghosh S. N. (1994) – Effect of a magnetic field on blood flow thorugh an indented tube in the presence of erythrocytes; Indian J. Pure Appl. Math. 25 345-352.
[7] Sneddon I.N. (1972) – The Use of Integral Transforms; University of Minnesota, Mc-Graw Hill.
[8] Shukla, J. B., Gupta, S. P., & Parihar, R. S. (1980). Biorheological aspects of blood flow through artery with mild stenosis : effects of peripheral layer. Biorheology, 17(5-6), 403–410.
[9] Srivastava, V. P. (2003). Flow of a couple stress fluid representing blood through stenotic vessels with a peripheral layer. Indian Journal of Pure and Applied Mathematics, 34(12), 1727-1740.
[10] Reddy, J. N., & Gartling, D. K. (2010). The finite element method in heat transfer and fluid dynamics. CRC press.